Title	Fast depth-sensitive fluorescence measurements in turbid media using cone shell configuration
Author(s)	Ong, Yi Hong; Liu, Quan
Citation	Ong, Y. H., & Liu, Q. (2013). Fast depth-sensitive fluorescence measurements in turbid media using cone shell configuration. Journal of Biomedical Optics, 18(11), 110503.
Date	2013
URL	http://hdl.handle.net/10220/18796
Rights	

Journal of Biomedical Optics

SPIEDigitalLibrary.org/jbo

Fast depth-sensitive fluorescence measurements in turbid media using cone shell configuration

Yi Hong Ong
Quan Liu

SPIE

Fast depth-sensitive fluorescence measurements in turbid media using cone shell configuration

Yi Hong Ong and Quan Liu
Nanyang Technological University, Division of Bioengineering, School of Chemical and Biomedical Engineering, Singapore 637457, Singapore

Abstract. Depth-sensitive fluorescence spectroscopy in a two-layered epithelial tissue phantom was demonstrated using a cone shell configuration implemented by an axicon lens and a fiber assembly including five rings of collection fibers. Each collection fiber ring was located at a different radial distance away from the center, for which fluorescence measurements from all rings showed a larger range of sensitivities to the top and bottom layers compared to the previously reported cone shell configuration. Furthermore, multiple fluorescence spectra corresponding to a range of successive targeted depths can be obtained simultaneously, which shortened data acquisition dramatically and eliminated the mechanical moving components required for depth-sensitive optical measurements in the previous setup. This new setup therefore would be preferred in a clinical setting.
[DOI: 10.1117/1.JBO.18.11.110503]

Keywords: depth-sensitive measurements; fluorescence spectroscopy; cone shell configuration; simultaneous spectra acquisition; turbid media.

Paper 130661LR received Sep. 12, 2013; revised manuscript received Oct. 22, 2013; accepted for publication Oct. 23, 2013; published online Nov. 18, 2013.

Autofluorescence spectroscopy in the ultraviolet/visible spectrum offers a noninvasive and effective approach for the detection of various epithelial cancers and precancers due to rich endogenous biological fluorophores in epithelial tissues that carry vital diagnostic information. As the depth distribution of these fluorophores is dependent on various factors such as age, menopausal status,[1] and progression of disease state,[2] the excellent capability of performing depth-sensitive fluorescence measurements in epithelial tissues would effectively improve the diagnostic performance of this technique. Achieving high depth sensitivity to a specific subsurface region in human epithelial tissue is a great challenge as photons will be quickly scattered when entering a tissue, i.e., a diffusively scattering medium. Furthermore, the dominance of fluorescence signals from overlying layers greatly reduces the contrast of fluorescence signals originated from the subsurface region of interest, thus limiting the diagnostic performance of this technique. To overcome this limitation, our group has previously introduced a noncontact axicon lenses-based setup with a cone shell configuration that exhibited enhanced depth sensitivity to subsurface layers and a larger range of sensitivity to both the top and bottom layers in an epithelial tissue phantom than that of a conventional convex lens-based setup with a cone configuration.[3] Moreover, the axicon lenses–based setup eliminates the need of moving the objective lens up or down, which is normally needed in a cone setup, to achieve depth-sensitive measurements. The setup effectively improves the consistency of optical coupling and thus would be preferred in a clinical setting. However, depth-sensitive measurements using this setup can be time inefficient as it still requires the change in the distance between two axicon lenses in the setup.

In this study, we increase the spectra acquisition speed of the axicon lenses–based setup by incorporating five rings of collection fibers into the detection configuration, which enables the collection of optical spectra from five different depths simultaneously. The new setup gets rid of the mechanical moving part consisting of two axicon lenses that are required to achieve depth-sensitive measurements. The performance of this new setup is evaluated in the same manner as in our previous report.[3]

The experimental setup including a fiber assembly with five rings of collection fibers was constructed as shown in Fig. 1(a). A 405-nm diode laser (iFlex-2000, Point Source Ltd., Hamble, UK) coupled to a single-mode fiber was used to deliver excitation light with a maximum output power of 30 mW. The output laser light was collimated using a convex lens ($f = 75.0$ mm) to achieve a beam with a diameter of 9 mm. Then the beam passed through a 405-nm laser line filter and a dichroic mirror before focusing on the sample by an axicon lens, with an apex angle of 110 deg. The axicon lens was fixed at a distance of 0.89 mm above the sample surface. The fluorescence signal was collected through the same axicon lens and passed through a long-pass filter before being imaged onto the tip of a custom designed fiber assembly [Leoni (SEA) Pte. Ltd., Singapore] by a convex lens ($f = 35.0$ mm). The distance between this imaging lens (IL) and the tip of the collection fiber assembly end B was adjusted to be 28.5 mm. Figures 1(b) and 1(c) show the arrangement of fibers on ends A and B of the fiber assembly, respectively. The fiber assembly consisted of 48 live fibers, represented by colored dots, and 43 dead spacer fibers, represented by black dots. These fibers were all identical with core/cladding/coating diameters of 100/110/125 μm and a numerical aperture of 0.22. Live fibers at end A of the fiber assembly were symmetrically arranged into five rings surrounding a central spacer fiber, in which the number of collection fibers was 6, 6, 12, 12, and 12, respectively, from the inner to the outer ring. At end B of the fiber assembly, these live fibers were arranged into five blocks each with six rows of fibers, and any two adjacent blocks of fibers were vertically separated by 530 μm. The first two blocks had one fiber in each row, while blocks 3, 4, and 5 had two fibers in each row, as shown in Fig. 1(c). From the top to the bottom of Fig. 1(c), the five blocks corresponded to rings 1, 2, 3, 4, and 5 in the order from the inner ring to the outer ring.

The fluorescence signals collected by the fiber assembly were directed to a Czerny–Turner type spectrograph (Shamrock 303, Andor Technology, Belfast, UK), which were equipped with

Address all correspondence to: Quan Liu, Nanyang Technological University, Division of Bioengineering, School of Chemical and Biomedical Engineering, Singapore 637457, Singapore. Tel: +65-65138298; Fax: +65-67911761; E-mail: quanliu@ntu.edu.sg.

0091-3286/2013/$25.00 © 2013 SPIE

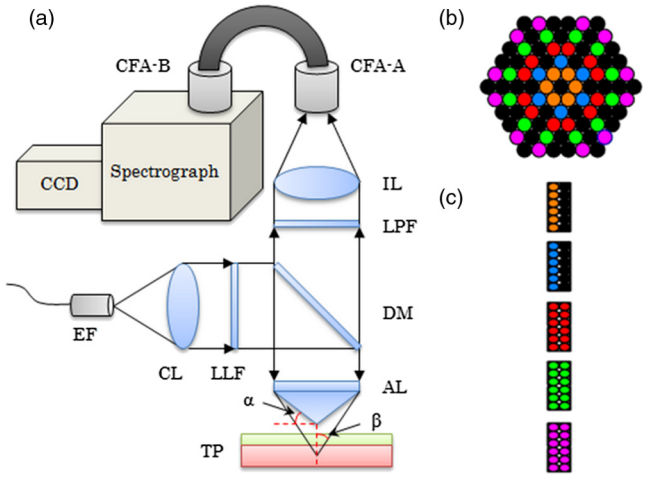

Fig. 1 (a) Schematic diagram of experimental setup: EF, excitation fiber; CL, collimating lens; LLF, laser line filter; DM, dichroic mirror; AL, axicon lens; LPF, longpass filter; IL, imaging lens; TP, tissue phantom; CFA, collection fiber assembly, (b) cross-section view of the collection fiber assembly on end A (CFA-A), and (c) cross-section view of the collection fiber assembly on end B(CFA-B). Black dots represent dead fibers for spacing while colored dots represent live fibers for light transmission in (b) and (c).

a holographic grating (1200 grove/mm) and a research-grade charge- coupled device (CCD) (DU920P-BR-DD, Andor Technology, Belfast, UK). The input slit of the spectrometer was set to be 250-μm wide in order to allow the signals from fiber assembly end B to enter, achieving a spectral resolution of 0.645 nm. The CCD was horizontally divided into five regions that were spaced apart vertically so that each region covered one block on the fiber assembly end B. Photons reaching each CCD region were binned vertically to produce five spectra corresponding to five individual fiber blocks for each measurement. The integration time for this experiment was always 0.5 s. The laser powers incident on the sample were measured to be 15 mW.

A two-layered agar phantom was fabricated using the recipe and procedure reported elsewhere.[4] flavin adenine dinucleotide (FAD) was added to the top layer at a concentration of 33.2 μM, whereas protoporpyrin IX (PpIX) was added to the bottom layer at a concentration of 32.3 μM. FAD and PpIX were chosen as the fluorophores for this study because they are intrinsic biological fluorophores that can be found inside tissues,[5] with nonoverlapping emission peaks at 525 and 630 nm, respectively. The dimension and optical properties of the phantom were made identically to our previous work.[3]

During measurements, the collected signals that reached the IL were focused onto the tip of fiber assembly end A with an approximate demagnification factor of 5.4. The axicon lens was lifted to 0.89 mm above the sample so as to prevent the superficial fluorescence signals from reaching the central dead fiber on the fiber assembly end A. Each ring of collection fibers on the collection fiber assembly corresponded to a different targeted depth in the tissue phantom. The corresponding depth in the phantom for each fiber ring was computed by Pythagoras theorem with the beam deviation angle, β given by:

$$\beta = \sin^{-1}(n \cdot \sin \alpha) - \alpha, \qquad (1)$$

Table 1 Radial distance of each ring of collection fibers from the center of fiber assembly, R_F; corresponding radial distance from the center of axicon lens, R_A; corresponding depth in phantom corrected for refractive index mismatch when lens-sample distance is 0 mm, D_P; and the corresponding depth in phantoms corrected for refractive index mismatch when lens-sample distance is 0.89 mm, D'_P.

Ring	R_F (mm)	R_A (mm)	D_P (mm)	D'_P (mm)
1	0.125	0.675	0.89	0.00
2	0.250	1.350	2.05	1.16
3	0.375	2.025	3.21	2.32
4	0.500	2.700	4.36	3.47
5	0.625	3.375	5.52	4.63

where the refractive index, n, of the axicon (N-BK7 glass) is 1.53 at 405 nm.[6] The corresponding depths of measurements for each ring of fibers, which were corrected for refractive index mismatch between the tissue phantom and the air, as described by Everall,[7] were shown in Table 1. The calculation was based on the refractive indices of air and intralipid 20% at 405 nm, which are 1 and 1.364,[8] respectively.

Figure 2 shows fluorescence spectra measured using the system shown in Fig. 1(a). Each spectrum was measured from a different ring of fibers, labeled by the ring number from 1 to 5, with an increasing distance from the assembly's center as shown in Table 1. FAD peak intensity that represents the fluorescence contribution from top layer increases from ring 1, which corresponds to the sample surface at 0 mm, to the maximum in ring 2, which corresponds to a targeted depth of 1.16 mm beneath the surface. FAD peak intensity then goes down from ring 3 to ring 4 and reaches the minimum in ring 5. PpIX peak intensity that represents the fluorescence contribution from the bottom layer increases significantly from ring 1 to ring 2 and reaches the maximum in ring 3 which corresponds to a targeted depth of 2.32 mm. Then, PpIX peak intensity starts to drop from ring 4 to ring 5. In both representative peak locations of FAD and PpIX, the peak intensity

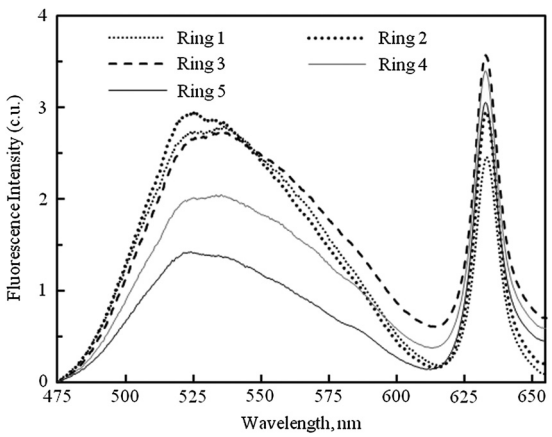

Fig. 2 Fluorescence spectra measured using different rings of collection fibers from the two-layered phantom. The abbreviation "c.u." refers to the calibrated unit.

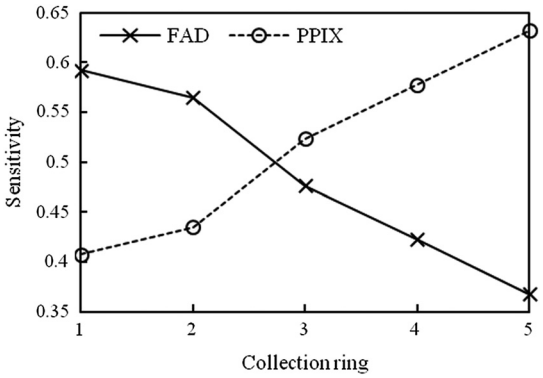

Fig. 3 Sensitivity of each collection ring to the top (FAD) and bottom (PpIX) layers of the tissue phantom.

increases to the maxima with an increasing targeted depth and then decreases after that. The same trend has been observed and discussed in our previous work.[3]

To evaluate the performance of this system in depth-sensitive measurements, we computed the sensitivities in fluorescence measurements to the top and bottom layers as described. First, the raw spectra measured by the ring 1 and ring 2 were multiplied by a ratio of 2, as the number of fibers in each of these rings was only half of the number of fibers in the outer three rings, so that the fluorescence intensities measured by all rings had similar magnitudes. Then, background spectrum was subtracted from each spectrum. After that, the FAD peak intensity measured by each ring was divided by the maximum of these peak intensities to get the normalized FAD intensities. Similarly, the PpIX peak intensity measured by each ring was divided by the maximum among these peak intensities to obtain the normalized PpIX intensities. The sensitivity of fluorescence measurements to the top layer was then computed by taking the ratio of the normalized FAD intensity measured by each ring to the sum of the normalized FAD and PpIX intensities measured by the same ring. The sensitivity of fluorescence measurements to the bottom layer was calculated by taking the ratio of the normalized PpIX intensity measured by each ring to the sum of the normalized FAD and PpIX intensities measured by the same ring.

Figure 3 shows the sensitivity of fluorescence measurements achieved by each collection ring in this system to the top and bottom layer of the tissue phantom. It can be seen that the sensitivity to the top layer (FAD) for collection ring 1 was the highest at 0.59, followed by collection ring 2 at 0.56, collection ring 3 at 0.48, collection ring 4 at 0.42, and the lowest by collection ring 5 at 0.37. On the other hand, the sensitivity to the bottom layer for collection ring 1 was the lowest at 0.41, followed by collection ring 2 at 0.44, collection ring 3 at 0.52, collection ring 4 at 0.58, and the maximum by collection ring 5 at 0.63. Compared to the top layer sensitivities for our previous axicon lenses–based setup[3] ranging from 0.36 to 0.53, which correspond to a targeted depth varying from 0 to 4.6 mm, the top layer sensitivities for the new setup varied from 0.37 (ring 5) to 0.59 (ring 1) for the same range in the targeted depth in this study. The sensitivities to the top layer at a targeted depth of 4.6 mm in both setups were similar but the maximum sensitivity to the top layer in the new setup was increased by ~11.3%. Consequently, the bottom layer sensitivities of the previous setup at the targeted depth of 0 and 4.6 mm were 0.47 and 0.64, whereas those of the new setup in this study were 0.41 and 0.63. This observation indicated the achievement of a larger range of sensitivity to the bottom layer by the incorporation of collection fibers in multiple rings to the detection configuration, for which the detailed explanation of the observation has been described previously.[3]

The ring illumination and detection configuration could be viewed as the superposition of multiple pairs of tilted source and detector fibers. As the ring diameter increases from ring 1 to ring 5, the source–detector separation increases, resulting in a monotonic change of sensitivity to the top or the bottom layers, which has been simulated in the literature.[9] The improvement in the maximum sensitivity to the top layer in the new setup compared to the previous setup could be attributed to the fact that the collection fibers in the inner ring in Fig. 1(b) served as a photon gate that blocks photons not originated from the targeted depth due to its limited numerical aperture. A similar gating mechanism did not exist in our previous setup thus a portion of those photons from the deep layer can be detected and cause degradation in the sensitivity to the top layer.

In this letter, we incorporated five rings of collection fibers into the detection part of an axicon lens based setup to detect optical spectra from five different depths simultaneously, which enables much faster spectral acquisition compared to our previous axicon lenses based setup. Moreover, the new setup has a higher sensitivity to the top layer and a larger range of sensitivities to both the top and bottom layers in a two-layered turbid phantom. Therefore this new setup would offer greater convenience and better diagnostic performance in clinical measurements.

Acknowledgments

The authors gratefully acknowledge financial support from the New Investigator Grant (Project No. NMRC/NIG/1044/2011) funded by the National Medical Research Council (NMRC) and a Tier 1 grant and Tier 2 grant funded by the Ministry of Education in Singapore (Grant Nos. RG47/09 and MOE 2010-T2-1-049).

References

1. M. Follen et al., "Effects of biographical variables on cervical fluorescence emission spectra," *J. Biomed. Opt.* **8**(3), 479–483 (2003).
2. R. Drezek et al., "Autofluorescence microscopy of fresh cervical-tissue sections reveals alterations in tissue biochemistry with dysplasia," *Photochem. Photobiol.* **73**(6), 636–641 (2001).
3. Y. H. Ong and Q. Liu, "Axicon lens-based cone shell configuration for depth-sensitive fluorescence measurements in turbid media," *Opt. Lett.* **38**(15), 2647–2649 (2013).
4. R. Cubeddu et al., "A solid tissue phantom for photon migration studies," *Phys. Med. Biol.* **42**, 1971–1979 (1997).
5. H. G. Breunig, H. Studier, and K. König, "Multiphoton excitation characteristics of cellular fluorophores of human skin *in vivo*," *Opt. Express* **18**(8), 7857–7871 (2010).
6. SCHOTT Optical Glass Data Sheet (2012), http://refractiveindex.info/.
7. N. Everall, "Modeling and measuring the effect of refraction on the depth resolution of confocal Raman microscopy," *Appl. Spectrosc.* **54**(6), 773–782 (2000).
8. H. F. Ding et al., "Determination of refractive indices of porcine skin tissues and intralipid at eight wavelengths between 325 and 1557 nm," *J. Opt. Soc. Am. A* **22**(6), 1151–1157 (2005).
9. I. V. Meglinski and S. D. Matcher, "Analysis of the spatial distribution of detector sensitivity in a multilayer randomly inhomogeneous medium with strong light scattering and absorption by the Monte Carlo method," *Opt. Spectrosc.* **91**(6), 654–659 (2001).